Inorganic Chemistry

Article

pubs.acs.org/IC

# Trinuclear and Tetranuclear Re(I) Rings Connected with Phenylene, Vinylene, and Ethynylene Chains: Synthesis, Photophysics, and Redox Properties

Jana Rohacova,[†,‡] Akiko Sekine,[§] Tsubasa Kawano,[§] Sho Tamari,[§] and Osamu Ishitani*[,†,‡]

[†]Department of Chemistry, Graduate School of Science and Engineering, Tokyo Institute of Technology, 2-12-1-NE-1 Ookayama, Meguro-ku, Tokyo 152-8550, Japan

[‡]CREST, Japan Science and Technology Agency, 4-1-8 Honcho, Kawaguchi-shi, Saitama 322-0012, Japan

[§]Department of Chemistry and Material Science, Graduate School of Science and Engineering, Tokyo Institute of Technology, 2-12-1-H60 Ookayama, Meguro-ku, Tokyo 152-8551, Japan

Supporting Information

**ABSTRACT:** A series of highly luminescent trinuclear and tetranuclear ring-shaped Re(I) complexes wherein the Re units are linked with rigid bidentate phosphine ligands, namely, bis(diphenylphosphino)-*p*-phenylene, -*trans*-vinylene, and -ethynylene, were synthesized and fully characterized. Their strong emissive properties and the long lifetimes of their triplet metal-to-ligand charge transfer excited states originate primarily from enhanced, rigidity-induced interligand interactions between the 2,2′-bipyridine (bpy) ligand and the phenyl groups of the phosphine ligands. In addition, another type of interligand interaction was also observed between the bpy ligand and the phosphine-bridging group; this interaction also strongly affected the photophysical and redox properties of the Re-rings.

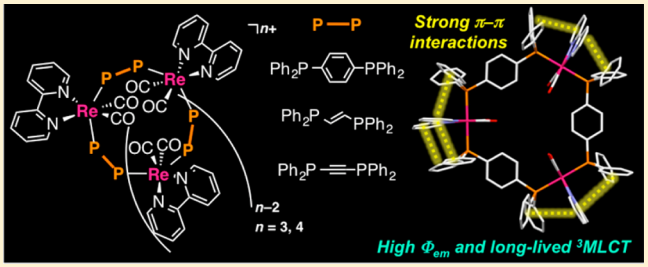


## INTRODUCTION

Transition-metal complexes exhibiting room-temperature luminescence from a low-lying, tunable metal-to-ligand charge transfer (MLCT) excited state[1] have been widely explored over the past several decades for their potential applications as luminescent probes for sensing and biological labeling, as electroluminescence devices, and in solar energy conversion processes as photocatalysts or dye-sensitized solar cells.[2−5] The *fac*-[$Re^{I}$(N^N)$(CO)_3$X] family (N^N = diimine; X = Cl or Br) occupies a prominent position in the photophysics and photochemistry of the MLCT-types complexes.[6−9] Previously, we reported the photochemical synthesis and photophysical properties of another series of biscarbonyl bisphosphine Re(I) complexes, *cis,trans*-[Re(N^N)$(CO)_2(PR_3)(PR'_3)$]$^+$, which when compared with *fac*-[$Re^{I}$(N^N)$(CO)_3$X] complexes exhibit more intense absorption in the visible region, improved emissive properties, and a longer-lived $^3$MLCT excited state.[10] Moreover, we observed that coordination of phosphine ligands with aryl groups induces interligand $\pi-\pi$ interactions between the diimine ligand and the aryl groups. These interactions result in unusual emissive and redox properties, i.e., a red-shift of absorption but a blue-shift of emission, a longer lifetime of the $^3$MLCT excited state, and stronger oxidation power in the $^3$MLCT excited state.[11,12]

Emissive polynuclear transition-metal complexes have also garnered attention as chromophoric and/or electroactive units because of their potential applications in light-harvesting and light-emitting devices and molecular-scale photonic wires.[13−16] We reported the synthesis of linear Re(I) oligonuclear and polynuclear complexes with *cis,trans*-[Re(N^N)$(CO)_2(PR_3)_2$]$^+$ as building blocks; these complexes can emit at room temperature even in solutions.[17] Because of the emissive and stable properties of the $^3$MLCT excited state of the linear Re(I) oligomers, they were successfully applied in artificial light-harvesting systems.[18,19]

Very recently, we also developed ring-shaped multinuclear Re(I) complexes that comprise a linkage of $Re^{I}$(N^N)$(CO)_2$ units with bidentate phosphine-alkyl ligands $PPh_2-(CH_2)_m-PPh_2$ ($m$ = 2−6) (**P−P**) (the structures of some examples are shown in Chart 1 as **R*n*e** and **R*n*b** for $m$ = 2 or 4, respectively).[20,21] Interestingly, some of these Re-rings exhibited outstanding photophysical and electrochemical properties and were more suitable as a redox photosensitizer, even compared with the corresponding linear multinuclear complexes and the mononuclear complexes *cis,trans*-[Re(N^N)$(CO)_2${$PPh_2(C_nH_{2n+1})$}$_2$]$^+$. These Re-rings exhibited longer lifetimes and greater oxidation power of the $^3$MLCT excited state as well as photochemical multielectron accumulation in a single molecule. Actually, the most efficient photocatalytic system for $CO_2$ reduction was successfully developed using one of the Re-rings as a redox photosensitizer

**Received:** June 22, 2015
**Published:** August 20, 2015





DOI: 10.1021/acs.inorgchem.5b01397
*Inorg. Chem.* 2015, 54, 8769−8777

**Chart 1. Structure and Abbreviations of the Trinuclear and Tetranuclear Re(I) Rings R*nx*[a]**

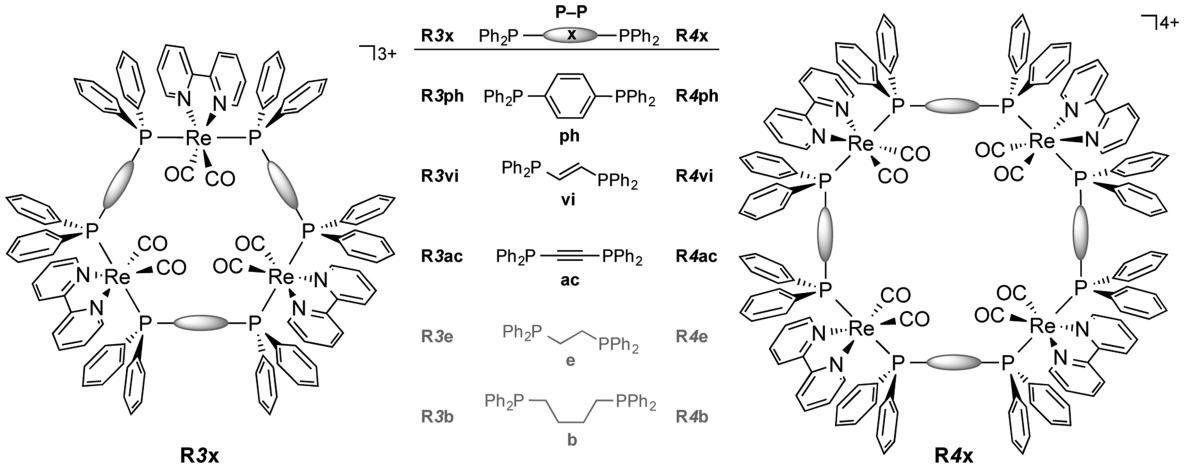


[a]All complexes were synthesized as $PF_6^-$ salts.

**Scheme 1. Synthesis of R3ph**

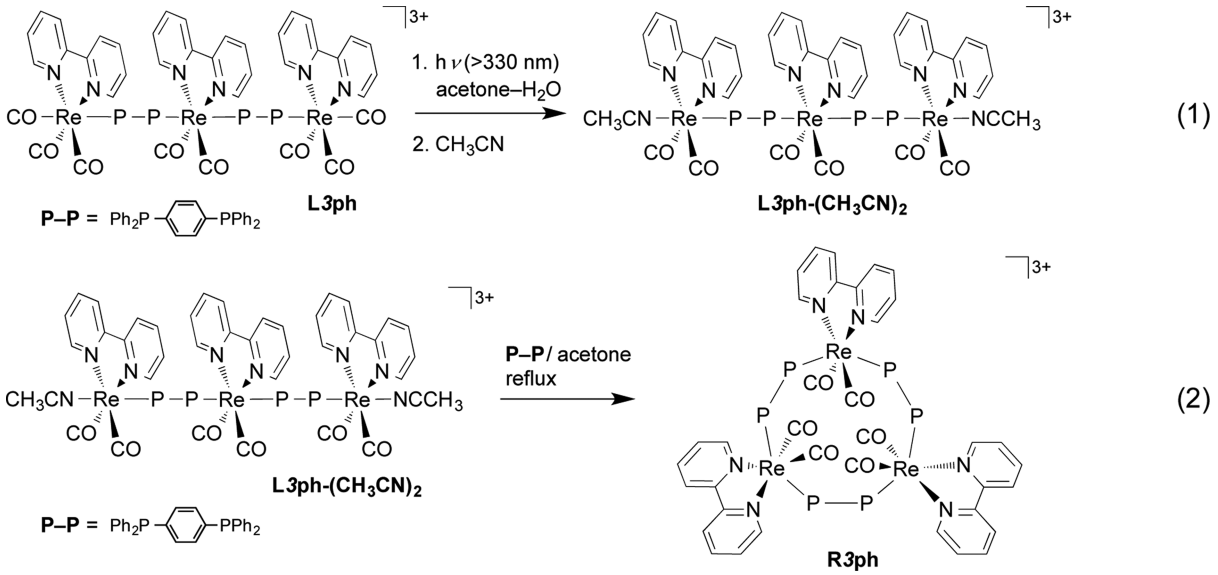


in conjunction with a catalyst.[20] Such fascinating properties were not observed in all of the Re-rings but only in Re-rings with a small inner cavity that was a consequence of the low number of metal units in the Re-ring and/or the short alkyl chain length of the bidentate phosphine-alkyl ligand **P−P**. In the Re-rings with such a smaller inner cavity, both the diimine ligands and the phenyl groups of the phosphine ligands are located outside the inner cavity by steric hindrance and are in close proximity to each other. Such steric restriction causes stronger interligand $\pi-\pi$ interactions.

Herein, we report new Re(I) rings constructed with **P−P** ligands whose two phosphine atoms are connected by an aromatic ring or a multiple bond instead of a flexible alkyl chain; in particular, they are connected by *p*-phenylene (**ph**), *trans*-vinylene (**vi**), or ethynylene (**ac**) spacers (Chart 1). All of them are highly emissive Re-rings, and the properties of their excited state are not significantly affected by the size of the inner cavity of the ring.

## RESULTS AND DISCUSSION

**Synthesis and Characterization.** Two methods for synthesizing Re-rings containing **P−P** ligands with a flexible alkyl spacer have been reported: oligomerization of dinuclear Re(I) complexes,[20] giving a mixture of Re-rings with various even numbers of the Re(I) units, and cyclization of the linear *n*-nuclear complex, selectively giving the corresponding Re-ring.[20,21] In this study, we chose the latter method because the number of Re(I) units in the target Re-rings should be limited because of the rigid structure of the employed **P−P** bridging ligands and because the former method would possibly give various linear oligomers and polymers as byproducts. Furthermore, given the geometric character of the bidentate phosphine ligand used in this work, i.e., the phosphorus tetrahedral angle and the hardly flexible spacer, we narrowed the synthesis to the trinuclear and tetranuclear motifs as feasible structures.

As a typical example, the synthesis of a trinuclear complex with the *p*-phenylene spacer (**R3ph**) is summarized in Scheme 1. The linear trinuclear Re(I) complex bearing the **ph** bridging



DOI: 10.1021/acs.inorgchem.5b01397
*Inorg. Chem.* 2015, 54, 8769−8777

ligands and two acetonitrile molecules as labile ligands at both edges (**L3ph-$(CH_3CN)_2$**) was synthesized using the photochemical ligand substitution reaction, as shown in eq 1.[10,22] An acetone solution containing **L3ph-$(CH_3CN)_2$** and an equivalent amount of **ph** was refluxed for 24 h, giving **R3ph** (eq 2), which could be isolated by size-exclusion chromatography;[23] the isolated yield was 47%. The same procedures were used to synthesize **R*n*vi** and **R*n*ac** ($n$ = 3, 4) in 30−40% yields. The exception was **R4ph**, which was produced with a significantly lower isolated yield (7%); we attributed this lower yield to the complex's steric and geometric factors.

All of the trimers and **R4ph** were analyzed by single-crystal X-ray diffraction; their crystal structures are shown in Figures 1−3 and Figures S1−S4 (Supporting Information, SI).

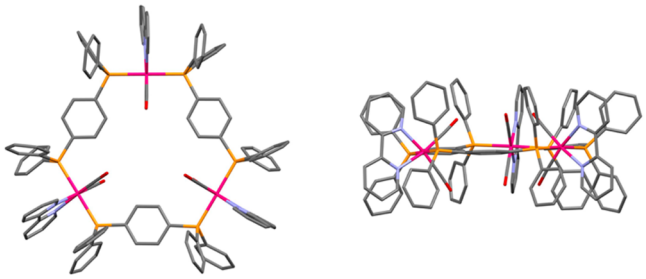

**Figure 1.** Molecular structure of **R3ph** (top and side views). Hydrogen atoms, $PF_6^-$, and solvent molecules are omitted for clarity. Gray, blue, red, orange, and pink correspond to C, N, O, P, and Re atoms, respectively.

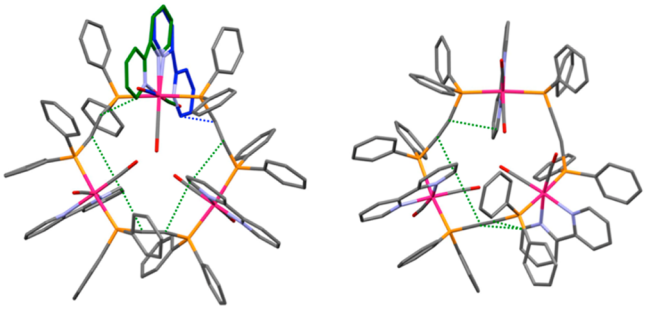

**Figure 2.** Molecular structures of **R3vi** (left) and **R3ac** (right), both from the top view. Disordered structures of one bpy ligand were observed in **R3vi** because of the ligand's special position, as indicated by the green or blue color of the bpy ligand, respectively. Hydrogen atoms, $PF_6^-$, and solvent molecules are omitted for clarity. Gray, blue, red, orange, and pink correspond to C, N, O, P, and Re atoms, respectively. Green (for both) and blue (for **R3vi**) dotted lines represent short distances between the bipyridyl ligands and vinylene or ethynylene chain of **P−P** within 3.5 Å (short distances between the bpy ligand and pendant phenyl groups are not displayed).

Interestingly, in the case of **R3ph** (Figure 1), all three bridging phenylene groups are fixed perpendicularly between the carbonyl ligands directed toward the inside of the inner cavity, whose interior diameter is ∼5.5 Å. This orientation provided an almost perfectly symmetrical hexagonal plane structure constructed among three sets comprising a Re(I) ion, a phosphine, a bridging phenylene, and another phosphine. Two pendant phenyl groups of **P−P** are located above the bpy ligand, which should induce strong $\pi-\pi$ interactions; the effects of these interactions on the properties of the Re-ring are discussed in a later section.

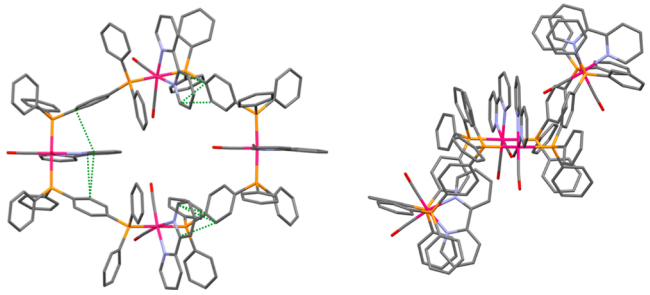

**Figure 3.** Molecular structure of **R4ph** (top and side views). Hydrogen atoms, $PF_6^-$, and solvent molecules are omitted for clarity. Gray, blue, red, orange, and pink correspond to C, N, O, P, and Re atoms, respectively. Green dotted lines represent short distances between the bipyridyl ligands and phenylene spacers of **P−P** within 3.5 Å (short distances between the bpy ligand and pendant phenyl groups are not displayed).

In the case of the other two trinuclear complexes (Figure 2), especially **R3ac**, the ring structure was squeezed and tightly packed, as clearly reflected in the more distorted P−Re−P angle, i.e., its distortion from linearity. The average angles were 173.4°, 175.2°, and 178.2° for **R3ac**, **R3vi**, and **R3ph**, respectively. In both **R3vi** and **R3ac**, the metal centers were accommodated outside one plane, and the inner cavities were much smaller (approximately 2.5 Å). In each metal unit of these two small Re-rings, one of the pendant phenyl groups of **P−P** was positioned between the CO ligands, probably because of steric hindrance among two phenyl groups and the bpy ligand. In all complexes, C−C distances shorter than the sum of the van der Waals radii (<3.5 Å) were observed between the bpy ligand and the phenyl group(s), demonstrating the presence of strong intramolecular $\pi-\pi$ interactions. Interestingly, in the cases of **R3vi** and **R3ac**, the distances between the carbon atoms of the bridging chain, i.e., vinylene and ethynylene, and the C6,C6′ atoms of the bpy ligands, were smaller than the sum of the van der Waals radii. Therefore, different types of intramolecular $\pi-\pi$ interactions may occur in these complexes.

The structure of **R4ph** (Figure 3) differs remarkably from that of the trinuclear analogue **R3ph** in that **R4ph** adopts a chairlike conformation with a shorter spatial distance between two opposite Re centers (10.6 Å) and a less distorted P−Re−P geometry (178.4°) compared with the other two Re ions with a significantly larger spatial distance (14.7 Å) and a more distorted angle (175.7°). The inner asymmetric cavity was observed to be slightly smaller (∼5 Å) than that of **R3ph**. The **R4ph** complex should preserve strong $\pi-\pi$ interligand interactions because two of the pendant phenyl groups and the bridging phenylene chain are located in close proximity to the bpy ligand.

Each Re−Re distance and Re−P−$C_{bridge}$ angle are compared in Table S2 (SI), and selected bond lengths and angles, together with distances between carbons within 3.5 Å, are summarized in Tables S3−S6 (SI).

Figure 4 displays the $^1$H NMR chemical shifts of the bpy protons of the synthesized Re-rings with the **ph**, **vi**, and **ac** bridging ligands; the chemical shifts of Re-rings with ethylene chains, i.e., $PPh_2-(CH_2)_2-PPh_2$, are included for reference. A single set of resonances clearly indicates that all of the Re-rings have highly symmetric structures on the NMR time scale. This symmetry is likely the result of rapid interconversion between some Re(I) conformations, as described later on the basis of FT-IR results. The bpy protons of **R3ph** and **R4ph** (Figure 4A)



DOI: 10.1021/acs.inorgchem.5b01397
*Inorg. Chem.* 2015, 54, 8769−8777

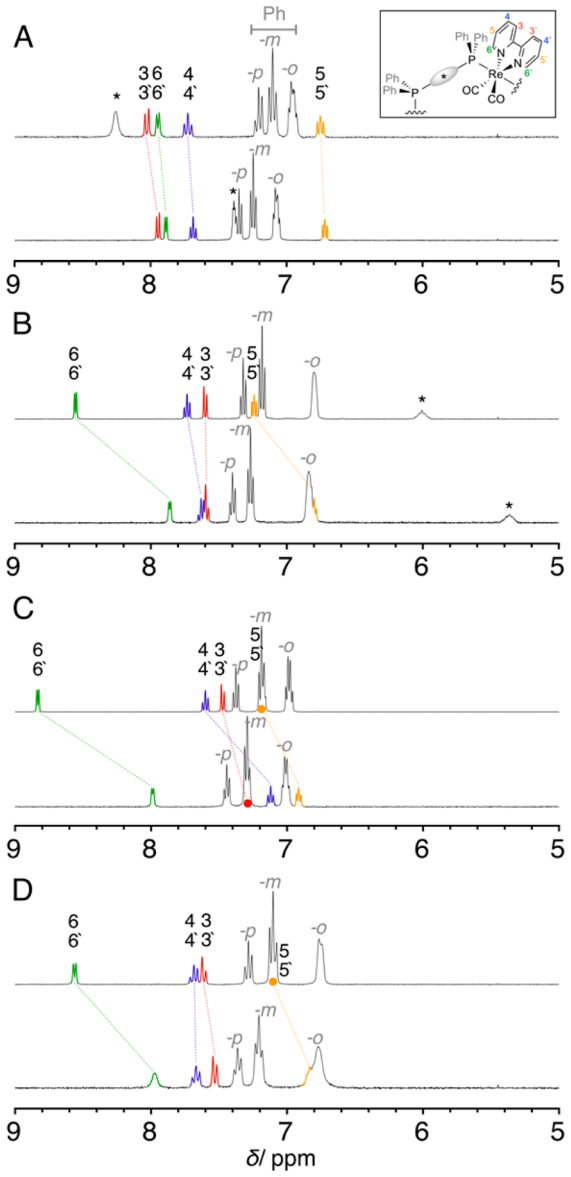


**Figure 4.** $^1$H NMR spectra of **R*n*ph** (A), **R*n*vi** (B), **R*n*ac** (C), and **R*n*e** (D) measured in $CD_3CN$: upper, ***n*** = 3; lower, ***n*** = 4. Numbers, letters, and * denominate bpy protons, P-phenyl groups, and **P−P** bridging-moiety protons, respectively, as represented schematically on one integrating unit.

were almost identical to each other, whereas the signals corresponding to the phenylene spacer were observed with different chemical shifts ($\delta$ = 8.3 ppm for **R3ph** and $\delta$ = 7.4 ppm for **R4ph**). Lower $\pi$-electron density around the phenylene spacer in the case of **R3ph** (the less-shielded signals) indicates that the phenylene groups do not easily access closer to the bpy ligands; i.e., the bpy ligands likely could not enter the inner space of the cyclic structure, in contrast to the case of **R4ph**, as was similarly indicated by the X-ray analysis results. In contrast, the similarity of the chemical shifts of the bpy protons in **R3ph**, **R4ph**, and the corresponding mononuclear complex *cis,trans*-$[Re(bpy)(CO)_2(PPh_3)_2]^+$ (**Reph$_2$**)[24] (Figure S5, SI), clearly demonstrates that strong $\pi-\pi$ interactions occurred between the phenyl groups and the bpy ligands; such interactions were also observed in the case of the similar mononuclear complex *cis,trans*-$[Re(dmb)(CO)_2(PAr_3)_2]^+$ (dmb = 4,4′-dimethyl-2,2′-bipyridyl).[11]

In contrast, the $^1$H NMR peaks of the bpy protons in the Re-rings with the **vi** or **ac** spacers (Figure 4B,C, respectively) revealed some substantial differences between the trinuclear and tetranuclear complexes; the bpy-6,6′-proton signals of **R3vi** and **R3ac** ($\delta \approx 8.7 \pm 0.1$ ppm) were remarkably downfield-shifted compared to those of **R4vi** and **R4ac** ($\delta \approx 8$ ppm). A similar trend but with a smaller difference was observed for the bpy-5,5′-protons ($\Delta\delta \approx 0.3-0.4$ ppm) of both series and for the bpy-4,4′-protons ($\Delta\delta \approx 0.5$ ppm) of the **ac** series. Such differences in the chemical shifts clearly indicate that the smaller inner cavities of **R3vi** and **R3ac** result in the bpy ligands and the phenyl groups being preferentially located in the outer positions of the inner cavity because a similar phenomenon was observed in the case of the ethylene-chain analogue **R*n*e** (Figure 4D).

The FT-IR spectra of the *cis,trans*-$[Re(bpy)(CO)_2(PR_3)(PR'_3)]^+$-type complexes measured in solution usually display two characteristic carbonyl peaks between 2000 and 1850 cm$^{-1}$ with similar intensities; these peaks correspond to the symmetric ($\nu_{sym}$) and asymmetric ($\nu_{asym}$) stretching modes, respectively. Interestingly, in the cases of the Re-rings, especially those of **R3vi**, **R3ac**, and **R4ac**, the $\nu_{asym}$ peaks were structured and/or broadened (Figure 5, measured in

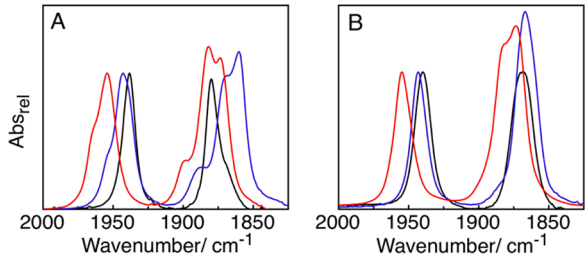


**Figure 5.** FT-IR spectra of **R3x** (A) and **R4x** (B) in $CH_3CN$; **x** = **ph** (black), **vi** (blue), and **ac** (red). The spectra were normalized to the absorbance of the symmetric peak maxima.

$CH_3CN$). This observation suggests the existence of different conformers of Re(I) units even in a single molecule of the Re-ring in solution; these conformers could not be distinguished on the NMR time scale as previously described, even at low temperature.[25] This broadening becomes less pronounced in the cases of the tetranuclear complexes when compared with the corresponding trinuclear complexes, and such remarkable differences in the IR spectra compared with those of the mononuclear Re(I) complexes were not observed in the cases of the Re-rings with the **ph** chains, where the inner cavities are larger than those in the other complexes. These results also indicate that the narrow inner space strongly restricts the entire structure of the Re-rings.

The $\nu$(CO) bands of **R*n*ac** were observed at higher frequencies when compared with those of the other rings, which is reasonably explained on the basis of the stronger $\pi$-acceptor character of the **ac** chain, which induces weaker Re−CO back-bonding and shortening of the CO bond length ($r_{CO}$). The bond lengths in solution can be calculated on the basis of the $\nu_{sym}$ and $\nu_{asym}$ peaks (or individual $\nu_{asym}$ peaks deconvoluted by Voigt fitting in the case of **R3vi**, **R3ac**, and **R4ac**) according to eq 3.[26] For the main conformer of the **R3ac** and **R4ac**, the $r_{CO}$ values were 1.150 and 1.151 Å, respectively. In contrast, the $r_{CO}$ values in the cases of **R3ph** and **R3vi** were both calculated as 1.152 Å, and in the cases of **R4ph** and **R4vi**, both were


DOI: 10.1021/acs.inorgchem.5b01397
*Inorg. Chem.* 2015, 54, 8769−8777

calculated as 1.153 Å. These C−O bond lengths were somehow shorter than those measured in the solid state ($r_{CO} \approx 1.16$ Å).

$$r_{CO} = 1.647 - 0.184 \ln k_{CO} \quad (k_{CO} \text{ in mdyn/Å}) \qquad (3)$$

**Electrochemical Properties.** Electrochemical studies provided clear evidence of mutual electronic communication among the units in some Re-rings. The cyclic voltammograms in Figure 6A show the first reduction waves for the trinuclear

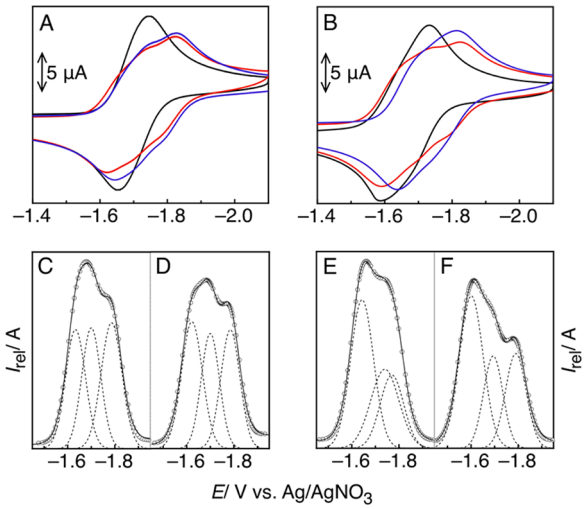


**Figure 6.** Cyclic voltammograms of **R3x** (0.5 mM) (A) and **R4x** (0.38 mM) (B) in DMF under Ar: sweep rate 100 mV $s^{-1}$; **x** = **ph** (black), **vi** (blue), and **ac** (red). Corresponding differential pulse voltammograms of **R3vi** (C), **R3ac** (D), **R4vi** (E), and **R4ac** (F) with the individual (---) and overall (○) Gaussian fits.

Re-rings, which correspond to the bpy-localized reduction (bpy/$bpy^{\bullet-}$). Although all of the processes were fully reversible, the shapes of the corresponding waves of **R3ph** and the other complexes differed substantially: the voltammogram for **R3ph** showed a single three-electron reduction wave, whereas stepwise one-electron reductions were observed for **R3vi** and **R3ac**. Thus, the corresponding differential pulse voltammetry (DPV) peaks (Figure 6C,D) more clearly confirmed an electrochemical nonequivalency of each center of **R3vi** and **R3ac** because the peaks required fitting with three Gaussian functions. Through-space electronic interactions occur among the three units in **R3vi** and **R3ac** because a similar phenomenon was also observed in the cyclic voltammogram and differential pulse voltammograms of **R3e** with ethylene chains (Figure S6, SI), whereas only minor DPV peak broadening was observed in the case of **R3b** with butyl chains and a wider inner ring cavity (Figure S6, SI). In the cases of the tetranuclear **R4vi** and **R4ac**, a similar electronic interaction was observed (Figure 6B). Even the first reduction wave of **R4ph** was slightly broadened (Figure 6B and Figure S7, SI) compared with that of **R3ph**. In the cases of **R4vi** and **R4ac**, the first largest peak in the deconvoluted differential pulse voltammogram was attributed to two-electron reduction, likely on the opposite sites, whereas the other two were one-electron reduction peaks (Figure 6E,F). However, as described in the previous cases of the corresponding trinuclear Re-rings, their differential pulse voltammograms could be separated into three peaks with similar peak areas. Two plausible factors may explain these electrochemical results: one is a difference of the inner cavities between the tetranuclear and trinuclear complexes, i.e., the spatial distances between each Re unit; the other is that the electronic interaction occurs only between adjacent Re units.

Figure 7 shows wider range cyclic voltammograms of **R3ph** and **R3ac** as typical examples; the voltammograms of the other

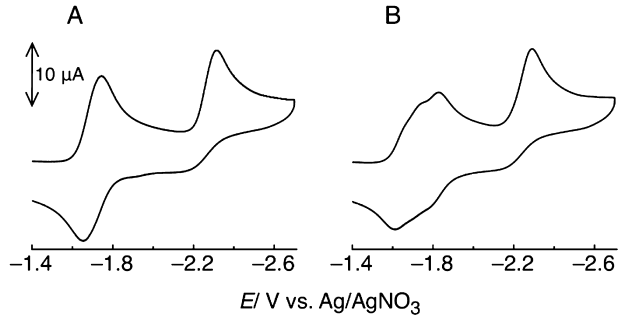


**Figure 7.** Full cyclic voltammograms (reduction scan) of **R3ph** (A) and **R3ac** (B) in DMF (both 0.5 mM) under Ar; sweep rate 100 mV $s^{-1}$.

complexes are shown in the Supporting Information (Figure S8, SI). The irreversible wave at approximately −2.3 V versus $Ag/AgNO_3$ is assigned to reduction of the metal center. In the oxidation sweep (Figure S9, SI), weak irreversible waves were observed at approximately 1.0 V versus $Ag/AgNO_3$, except in the case of the **ac**-based rings; these waves usually correspond to oxidation of the metal in this type of complex.[24] The absence of the oxidation peak within the solvent working window (up to 1.2 V vs $Ag/AgNO_3$) for **R*n*ac** is in agreement with the stronger $\pi$-acceptor character of the acetylene **P**−**P** moiety, as previously discussed; this stronger $\pi$-acceptor character facilitates $\pi$-back-bonding and increases the effective positive charge on the Re center. The metal-centered oxidation of Re(I) to Re(II) indeed becomes a less feasible process. The electrochemical results are summarized in Table 1.

**Photophysical Properties.** The UV−vis absorption spectra of the Re-rings measured in DMF exhibited a pattern typical of Re(I)-diimine derivatives, i.e., an interligand transition of the bpy ligands at $\lambda_{abs} \approx 300$ nm and an Re(d$\pi$) → bpy($\pi^*$) $^1$MLCT transition at longer wavelengths of approximately 400 nm (Figure 8). The highest-energy MLCT absorption was observed for the **R*n*ac** series, whereas the lowest was observed for the **R*n*ph** series. In contrast, only minor perturbations in the MLCT absorption maxima related to the ring size were observed in all of the members of the Re-ring series. Notably, the absorption maxima of **R*n*ac** and **R*n*vi** were blue-shifted compared with those of the corresponding Re-rings with a saturated alkyl chain **R*n*e** (Figure S10, SI).

Figure 9 shows the emission spectra of the Re-rings, all of which were strongly emissive at room temperature, even in solution. The broad and nonvibrational shape is typical of emission from the lowest $^3$MLCT excited state of the Re(I) complexes. **R*n*ac** (red) exhibited the highest-energy maxima at 581 ± 1 nm, and those of **R*n*vi** (blue) and **R*n*ph** (black) were red-shifted to 603 ± 1 and 612 ± 1 nm, respectively. The number of Re units also did not significantly affect the emission maximum in the cases of **R*n*ac**, **R*n*vi**, and **R*n*ph** ($\Delta\lambda_{em}$ = 1−3 nm), in contrast to the case of **R*n*e** ($\Delta\lambda_{em}$ = 5 nm). Table 1 summarizes the photophysical properties of the Re-rings. It is noteworthy that the emission quantum yields ($\Phi_{em}$) of **R*n*ac**, **R*n*vi**, and **R*n*ph** were much higher than those of the Re-rings with alkyl chains, even when compared with the $\Phi_{em}$ of **R*n*e**, which are relatively highly emissive among the Re-rings with


DOI: 10.1021/acs.inorgchem.5b01397
*Inorg. Chem.* 2015, 54, 8769−8777

**Table 1. Photophysical and Electrochemical Properties of the Rings Measured in DMF at 25°C**

| | $\lambda_{abs}$[a]/nm ($\varepsilon/10^3$ $M^{-1}$ $cm^{-1}$) | $\lambda_{em}$[b]/nm | $\tau_{em}$[c]/$\mu$s (%)[d] | $\Phi_{em}$[b] | $k_r$[e]/$10^5$ $s^{-1}$ | $k_{nr}/10^6$ $s^{-1}$ | $\Delta G°_{MLCT}$[f]/eV | $-E_{red}$[g]/V ($ne^-$)[h] |
|---|---|---|---|---|---|---|---|---|
| **R3ph** | 403 (10.7) | 612 | 0.89 | 0.08 | 0.90 | 1.03 | 2.69 | 1.68 (3) |
| **R4ph** | 407 (11.1) | 613 | 0.85 | 0.05 | 0.59 | 1.12 | 2.67 | 1.60 (2) |
| | | | | | | | | 1.69 (2) |
| **Reph$_2$** | 408 (4.2) | 617 | 0.67 | 0.05 | 0.75 | 1.42 | 2.67 | 1.71 |
| **R3vi** | 392 (10.2) | 605 | 0.57 | 0.07 | 1.23 | 1.63 | 2.68 | 1.63 |
| | | | | | | | | 1.70 |
| | | | | | | | | 1.79 |
| **R4vi** | 396 (11.9) | 602 | 0.61 | 0.08 | 1.31 | 1.51 | 2.69 | 1.64 (2) |
| | | | | | | | | 1.74 |
| | | | | | | | | 1.77 |
| **R3ac** | 378 (10.1) | 583 | 0.86 | 0.16 | 1.86 | 0.98 | 2.74 | 1.62 |
| | | | | | | | | 1.70 |
| | | | | | | | | 1.78 |
| **R4ac** | 376 (11.0) | 580 | 0.74 | 0.15 | 1.96 | 1.16 | 2.76 | 1.60 (2) |
| | | | | | | | | 1.69 |
| | | | | | | | | 1.79 |
| **R3e** | 411 (10.7) | 617 | 0.74 (93) | 0.046 | | | 2.69 | 1.67 |
| | | | 0.15 (7) | | | | | 1.72 |
| | | | | | | | | 1.79 |
| **R4e** | 400 (12.0) | 612 | 0.54 (96) | 0.049 | | | 2.64 | 1.66 (2)[j] |
| | | | 0.18 (4) | | | | | 1.76 (2)[j] |

[a]MLCT band. [b]$\lambda_{ex}$ = 400 nm. [c]$\lambda_{ex}$ = 401 nm. [d]In the case of plural lifetimes. [e]Radiative decay rate constant ($k_r = \Phi_{em}/\tau_{em}$). [f]Free energy of the MLCT excited state estimated from Franck−Condon analysis.[27] [g]First reduction potential vs $Ag/AgNO_3$, determined from the DPV peaks. [h]Unless $n > 1$. [j]From ref 21.

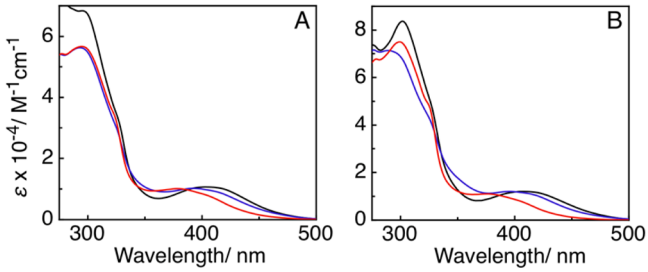


**Figure 8.** UV−vis spectra of **R3x** (A) and **R4x** (B) in DMF; **x** = **ph** (black), **vi** (blue), and **ac** (red).

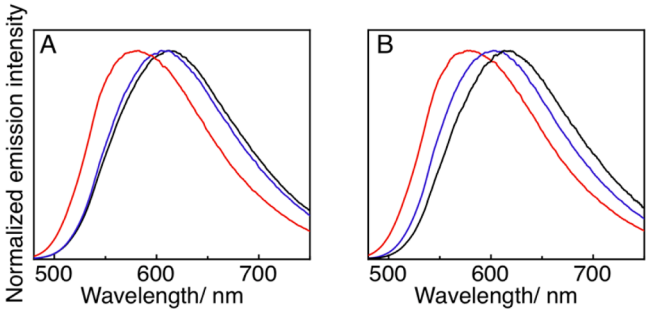


**Figure 9.** Normalized emission spectra of **R3x** (A) and **R4x** (B) in deaerated DMF at $\lambda_{ex}$ = 400 nm; **x** = **ph** (black), **vi** (blue), and **ac** (red).

the alkyl chains. In particular, the $\Phi_{em}$ of **R3ac** and **R4ac** were 0.16 and 0.15, respectively, which were approximately 3-fold larger than those of **R*n*e**. The emission decays measured using the single-photon counting method with $\lambda_{ex}$ = 401 nm could be fitted with a single exponential function with a long lifetime (0.57−0.89 $\mu$s) in all of the cases of **R*n*ph**, **R*n*vi**, and **R*n*ac**. Fitting these emission decays with a single exponential function is one of the marked differences from the Re-rings with alkyl spacers, whose emission decays were fitted using double exponential functions with lifetimes of 0.54−0.74 and 0.15−0.18 $\mu$s (Table 1). The origin of these plural emission lifetimes of the Re-rings with alkyl chains is attributed to different conformers with different strengths of $\pi-\pi$ interactions between the phenyl groups of the phosphine ligands and the bpy ligand; i.e., the conformer with the longer lifetime exhibits stronger $\pi-\pi$ interactions. Although we observed some conformers of the Re(I) unit in some cases of **R*n*ph**, **R*n*vi**, and **R*n*ac** in their IR spectra, the monotonic emission decays in all the cases strongly suggest that not only the phenyl groups but also the vinylene and ethynylene chains in the **P**−**P** ligand can interact with the bpy ligand, giving $\pi-\pi$ interactions, as observed in the aforementioned X-ray analysis results. These $\pi-\pi$ interactions also improve the photophysical properties, resulting in the longer lifetime and the higher emission quantum yield compared with those of the Re-rings with alkyl chains.

A comparison of the photophysical properties between **R*n*ph** and the corresponding mononuclear compound **Reph$_2$**, which also exhibits strong interligand $\pi-\pi$ interactions between the bpy ligand and the phenyl groups of the $PPh_3$ ligand, should be interesting. The emission lifetimes of the Re-rings were ca. 0.2 $\mu$s longer, although the absorption and emission maxima were only blue-shifted by a few nanometers (Table 1). The nonradiation decay rate constants ($k_{nr}$) of the **R*n*ph**, as calculated using eq 4, were smaller than those of **Reph$_2$** (Table 1), likely because of both the energy gap law[22,27] and the rigidity of the rings.

$$k_{nr} = (1 - \Phi_{em})/t_{em} \quad (4)$$



DOI: 10.1021/acs.inorgchem.5b01397
*Inorg. Chem.* 2015, 54, 8769−8777

## CONCLUSIONS

Novel tri- and tetranuclear ring-shaped Re(I) complexes bearing a bidentate phosphine ligand linked with phenylene, vinylene, or ethynylene chains were synthesized in good yields. These Re-rings exhibited strong interligand $\pi-\pi$ interactions not only between the bpy ligands and the phenyl groups of the phosphine ligands but also between the bpy and the connecting chains, i.e., the vinylene, ethynylene, and phenylene groups. These strong interligand $\pi-\pi$ interactions remarkably improved the properties of the Re-rings as emitters and likely as photosensitizers.

## EXPERIMENTAL PROCEDURE

**Materials and Methods.** Dry tetrahydrofuran (THF) was obtained by filtration through drying columns on a GlassContour solvent dispensing system (Nikko Hansen and Co. Ltd.). Dimethylformamide (DMF) was dried over molecular sieves 4 Å and distilled under reduced pressure and stored under Ar before use. Other anhydrous solvents were purchased from commercial sources.

All reactions were carried out under an inert atmosphere and dry conditions unless noted. Column chromatography was performed with silica gel 60 (40−50 μm, Kanto Chemical Co.). $Re_2(CO)_{10}$, *trans*-1,2-bis(diphenylphosphino)ethylene (**vi**), 1,2-bis(diphenylphosphino)-acetylene (**ac**), 2,2′-bipyridine, and other commercially available reagents were purchased from Kanto Chemical Co., Tokyo Kasei Co., Wako Pure Chemical Industries, and Aldrich Chemical Co., and used as received. *p*-Bis(diphenylphosphino)benzene (**ph**) was synthesized according to the literature.[28] All intermediates and multinuclear linear Re(I) complexes, such as *fac*-[Re(bpy)$(CO)_3$-$\eta^1$-ac]$^+$, **L3ac**, and **L4ac**, were synthesized according to the literature.[17] Similarly, the new complexes such as *fac*-[Re(bpy)$(CO)_3$-$\eta^1$-ph]$^+$, *fac*-[Re(bpy)$(CO)_3$-$\eta^1$-vi]$^+$, **L2ph**, **L2vi**, **L3ph**, **L3vi**, **L4ph**, and **L4vi** were synthesized according to the same procedure, and their characterization is reported hereafter. The Re(I) rings were synthesized according to the reported method.[21] All complexes were obtained as $PF_6^-$ salts.

Photochemical reactions were performed with a 500 W high-pressure mercury lamp EHBWI (Eikosha) with an uranium glass filter (>330 nm) in a Pyrex donut-form cell, and with bubbling of $N_2$ gas. During irradiation, both the reaction vessel and the light source were cooled with tap water. When necessary, separation of the complexes was achieved by size exclusion chromatography (SEC) using a pair of Shodex PROTEIN KW-2002.5 columns (300 mm × 20.0 mm i.d.) with a KW-LG guard-column (50 mm × 8.0 mm i.d.) and a JAI LC9204 recycling preparative HPLC apparatus (Japan Analytical Industry Co.) with a JASCO UV-2075Plus UV detector. The eluent was MeOH−$CH_3CN$ 1:1 (v/v) containing $CH_3COONH_4$ (0.15 M), and the flow rate was 6.0 mL min$^{-1}$.[23] $^1$H NMR, $^{13}$C NMR, and $^{31}$P NMR spectra were acquired with a JEOL AL300, JEOL AL400, JEOL ECX400, or JEOL ECA400II spectrometer. Chemical shifts ($\delta$/ppm) were referenced to residual $^1$H and $^{13}$C signals of the deuterated solvent ($^1$H, 1.94 ppm for $CD_3CN$, 2.05 ppm for $CD_3COCD_3$; $^{13}$C, 1.3 ppm for $CD_3CN$) and $^{31}$P signal of $PF_6^-$ (−145 ppm), respectively. All NMR spectra were recorded at room temperature, unless stated. Electrospray ionization mass spectrometry (ESI-MS) was conducted on a Shimadzu LCMS-2010A mass spectrometer. Electrospray ionization time-of-flight mass spectrometry (ESI-TOFMS) was undertaken with a Waters LCT Premier instrument. X-ray crystallographic data were collected at −100 °C for **R3ph**, **R3vi**, and **R3ac**, and −180 °C for **R4ph** on Rigaku R-AXIS RAPID-II with VariMax007 Mercury CCD systems with graphite monochromated Cu K$\alpha$ radiation ($\lambda$ = 1.541 86 Å). The sample crystals were yellow prisms. The structures of **R3ph**, **R3vi**, and **R3ac** were solved using the SHELXS97[29] programs, and that of **R4ph** was solved by the SHELXT[30] program. All structures were refined by the full-matrix least-squares method (SHELXL2014).[30] Non-hydrogen atoms were refined anisotropically, and hydrogen atoms were generated geometrically and refined using a riding model. CCDC 1407198, 1407199, 1407197, and 1407200 for **R3ph**, **R3vi**, **R3ac**, and **R4ph**, respectively, contain the supporting crystallographic data for this paper, which can be obtained free of charge from the Cambridge Crystallographic Data Centre via www.ccdc.cam.ac.uk/data_request/cif. FT-IR spectra were recorded with a JASCO FT/IR-610 spectrometer at 1 cm$^{-1}$ resolution with a TGS detector. Electrochemical voltammetric techniques were performed using a CHI720D electrochemical analyzer (CH Instruments, Inc.) with a glassy-carbon working electrode (diameter 3 mm), an $Ag/AgNO_3$ (10 mM) reference electrode, and an Pt counter electrode. The supporting electrolyte was $Et_4NBF_4$ (0.1 M), which was dried in vacuum at 100 °C for 1 day prior to use. UV−vis absorption spectra were recorded with a JASCO V-565 or V-670 spectrophotometer. Emission spectra were recorded at 25 °C using a JASCO FP-6500 spectrofluorometer and corrected for PMT response. Emission quantum yields were determined with a calibrated integrating sphere (Absolute PL Quantum Yield Measurement System C9920-01, Hamamatsu Photonics k.k.), comprising Xe lamp as an excitation source and a multichannel spectrometer (C10027).[31] Emission lifetimes were obtained at 25 °C using a HORIBA FluoroCube time-correlated single-photon counting system. The excitation light source was a NanoLED-405L (401 nm, <200 ps). All measurements were performed in Ar-saturated solutions, and the absorbance was adjusted at $\lambda_{ex}$ to ≈0.1.

**Syntheses.** *[Re(bpy)$(CO)_3$($\eta^2$-ph)Re(bpy)$(CO)_3$]$(CF_3SO_3)_2$* ***(L2ph).*** *fac*-[Re(bpy)$(CO)_3$OTf] (0.42g, 0.73 mmol) and *p*-bis(diphenylphosphino)benzene (0.16 g, 0.36 mmol) were refluxed in THF (25 mL) in dim light for 3 days. A pale yellow precipitate was filtered off, washed with ether, and dried in vacuum (0.5 g, 86%). For NMR and FT-IR characterization, **L2ph** was converted into $PF_6^-$ salt as follows. The solid was dissolved in a small amount of the MeOH−$CH_3CN$ mixture, and then a few drops of a saturated aqueous solution of $NH_4PF_6$ were added slowly giving light-yellow crystals. They were collected, washed with $H_2O$, and dried under vacuum.

$^1$H NMR (400 MHz, $CD_3COCD_3$): $\delta$ 8.83 (d, 4H, $J$ = 5.6 Hz, bpy-6,6′), 8.49 (d, 4H, $J$ = 8.4 Hz, bpy-3,3′), 8.18 (dd, 4H, $J$ = 8.8, 7.6 Hz, bpy-4,4′), 7.54 (m, 4H, Ph-*p*), 7.48 (m, 12H, bpy-5,5′ + Ph-*m*), 7.36 (dd, 4H, $J$ = 7.6, 4.8 Hz, P−$C_6H_4$−P), 7.25 (m, 8H, Ph-*o*) ppm. $^{31}$P NMR (161 MHz): $\delta$ 17.9 (*P*−$C_6H_4$−*P*) ppm. FT-IR ($CH_3CN$): $\nu$(CO) 2043, 1957, 1926 cm$^{-1}$. ESI-MS ($CH_3CN$): $m/z$ 650 [M − $2PF_6$]$^{2+}$.

*fac-[Re(bpy)$(CO)_3$-$\eta^1$-ph]$(CF_3SO_3)$* ***(Reph).*** *fac*-[Re(bpy)$(CO)_3$OTf] (0.3 g, 0.52 mmol) and *p*-bis(diphenylphosphino)benzene (1.16 g, 2.61 mmol) were refluxed in THF (100 mL) under inert atmosphere in dim light for 2 days. The solvent was removed under reduced pressure, and the crude solid was purified on column chromatography ($SiO_2$, $CH_3CN$−$CH_2Cl_2$ 1:5) to afford 0.2 g of yellow solid (38%). ESI-MS ($CH_3CN$): $m/z$ 873 [M − OTf]$^+$.

*[Re(bpy)$(CO)_3$($\eta^2$-ph)Re(bpy)$(CO)_2$($\eta^2$-ph)Re(bpy)$(CO)_3$]$(PF_6)_3$* ***(L3ph).*** **L2ph** (0.25 g, 0.16 mmol) was irradiated for 30 min in degassed $CH_2Cl_2$ (300 mL). After evaporation of the solvent, the crude red solid was dissolved together with **Reph** (0.2 g, 0.2 mmol) in THF (25 mL), and the mixture was heated under reflux in dim light for 24 h. Solvent was evaporated and the crude material purified by SEC. The fraction containing **L3ph** was collected, evaporated, and partitioned between $CH_2Cl_2$ and a $NH_4PF_6$ aqueous solution. The organic layer was washed once more with an aqueous $NH_4PF_6$ solution, dried over $Na_2SO_4$, and evaporated. Final recrystallization from EtOH−$CH_2Cl_2$ afforded the desired compound as yellow crystals (0.2 g, 48%).

$^1$H NMR (400 MHz, $CD_3COCD_3$): $\delta$ 8.79 (d, 4H, $J$ = 5.6 Hz, $bpy_{ex}$-6,6′), 8.47 (d, 4H, $J$ = 8.0 Hz, $bpy_{ex}$-3,3′), 8.23 (d, 2H, $J$ = 8.0 Hz, $bpy_{in}$-3,3′), 8.17 (dd, 4H, $J$ = 8.4, 7.6 Hz, $bpy_{ex}$-4,4′), 7.99 (d, 2H, $J$ = 5.6 Hz, $bpy_{in}$-6,6′), 7.78 (dd, 2H, $J$ = 8.0, 7.2 Hz, $bpy_{in}$-4,4′), 7.52 (m, 4H, $P_{ex}$Ph-*p*), 7.48−7.16 (m, 48H, $P_{in}$Ph-*p* + Ph-*m* + P−$C_6H_4$−P + Ph-*o* + $bpy_{ex}$-5,5′), 6.73 (dd, 2H, $J$ = 7.2, 5.6 Hz, $bpy_{in}$-5,5′) ppm. $^{31}$P NMR (161 MHz): $\delta$ 21.3 ($P_{ex}$−$C_6H_4$−$P_{in}$), 17.7 ($P_{ex}$−$C_6H_4$−$P_{in}$) ppm. FT-IR ($CH_3CN$): $\nu$(CO) 2043, 1956, 1942 1925, 1872 cm$^{-1}$. ESI-MS ($CH_3CN$): $m/z$ 714 [M − $3PF_6$]$^{3+}$.

*[Re(bpy)$(CO)_3${($\eta^2$-ph)Re(bpy)$(CO)_2$}$_2$($\eta^2$-ph)Re(bpy)$(CO)_3$]$(PF_6)_4$* ***(L4ph).*** **L2ph** (250 mg, 0.16 mmol) was irradiated for 30 min in


DOI: 10.1021/acs.inorgchem.5b01397
Inorg. Chem. 2015, 54, 8769−8777

degassed $CH_2Cl_2$ (300 mL). After evaporation of the solvent, the crude red solid was dissolved together with *p*-bis(diphenylphosphino)-benzene (35 mg, 0.08 mmol) in THF (15 mL), and the mixture was heated under reflux in dim light for 2 days. Solvent was evaporated and the crude material purified by SEC. The fraction containing **L4ph** was collected, evaporated, and partitioned between $CH_2Cl_2$ and a $NH_4PF_6$ aqueous solution. The organic layer was washed once more with an aqueous $NH_4PF_6$ solution, dried over $Na_2SO_4$, and evaporated, affording the desired compound as orange solid (90 mg, 31%).

$^1$H NMR (400 MHz, $CD_3CN$): $\delta$ 8.55 (d, 4H, $J$ = 5.6 Hz, $bpy_{ex}$-6,6′), 8.09 (d, 4H, $J$ = 8.0 Hz, $bpy_{ex}$-3,3′), 7.93 (dd, 4H, $J$ = 8.4, 7.6 Hz, $bpy_{ex}$-4,4′), 7.85 (d, 4H, $J$ = 8.0 Hz, $bpy_{in}$-3,3′), 7.72 (d, 4H, $J$ = 5.6 Hz, $bpy_{in}$-6,6′), 7.49 (dd, 4H, $J$ = 8.0, 7.6 Hz, $bpy_{in}$-4,4′), 7.44 (m, 4H, $P_{ex}$Ph-*p*), 7.40−7.25 (m, 32H, $P_{in}$Ph-*p* + Ph-*m*), 7.21 (dd, 4H, $J$ = 7.6, 5.6 Hz, $bpy_{ex}$-5,5′), 7.17−6.97 (m, 36H, P−$C_6H_4$−P + Ph-*o*), 6.39 (dd, 4H, $J$ = 7.2, 5.6 Hz, $bpy_{in}$-5,5′) ppm. $^{31}$P NMR (161 MHz): $\delta$ 21.7 ($P_{ex}$−$C_6H_4$−$P_{in}$), 18.1 ($P_{ex}$−$C_6H_4$−$P_{in}$) ppm. FT-IR ($CH_3CN$): $\nu$(CO) 2043, 1956, 1942 1925, 1872 cm$^{-1}$. ESI-MS ($CH_3CN$): $m/z$ 747 [M − $4PF_6$]$^{4+}$.

*[Re(bpy)(CO)$_3$($\eta^2$-vi)Re(bpy)(CO)$_3$](CF$_3$SO$_3$)$_2$* ***(L2vi)***. This compound was synthesized according to the same procedure as for **L2ph**. Starting from *fac*-[Re(bpy)(CO)$_3$OTf] (0.56g, 0.97 mmol) and *trans*-bis(diphenylphosphino)ethylene (0.2 g, 0.48 mmol), the target **L2vi** was obtained as light-yellow solid (0.64 g, 86%). For NMR and FT-IR characterization, **L2vi** was converted into $PF_6^-$ salt as was **L2ph**.

$^1$H NMR (300 MHz, $CD_3COCD_3$): $\delta$ 8.76 (d, 4H, $J$ = 5.4 Hz, bpy-6,6′), 8.37 (d, 4H, $J$ = 8.2 Hz, bpy-3,3′), 8.21 (dd, 4H, $J$ = 8.2, 7.7 Hz, bpy-4,4′), 7.66−7.57 (m, 8H, bpy-5,5′ + Ph-*p*), 7.48 (ddd, 8H, $J$ = 7.6, 7.3, 3.2 Hz, Ph-*m*), 7.01 (dd, 8H, $J$ = 8.5, 7.6 Hz, Ph-*o*), 5.91 (m, 2H, P—C*H*═C*H*—P) ppm. FT-IR ($CH_3CN$): $\nu$(CO) 2044, 1958, 1927 cm$^{-1}$. ESI-MS ($CH_3CN$): $m/z$ 625 [M − $2PF_6$]$^{2+}$.

*fac-[Re(bpy)(CO)$_3$-$\eta^1$-vi](PF$_6$)* ***(Revi)***. This compound was synthesized according to the same procedure as for **Reph**. Starting from *fac*-[Re(bpy)(CO)$_3$($CH_3CN$)]($PF_6$) (0.3 g, 0.49 mmol) and *trans*-bis(diphenylphosphino)ethylene (0.97 g, 2.45 mmol), the target **Revi** was obtained as yellow solid (0.3 g, 63%). ESI-MS ($CH_3CN$) $m/z$ 823 [M − $PF_6$]$^+$.

*[Re(bpy)(CO)$_3$($\eta^2$-vi)Re(bpy)(CO)$_2$($\eta^2$-vi)Re(bpy)(CO)$_3$](PF$_6$)$_3$* ***(L3vi)***. This complex was synthesized according to the same procedure as for **L3ph**. Starting from **L2vi** (0.33 g 0.21 mmol), and coupling with **Revi** (0.3 g, 0.32 mmol) after the irradiation, the target **L3vi** was obtained as yellow crystals (0.36 g, 68%).

$^1$H NMR (400 MHz, $CD_3COCD_3$): $\delta$ 8.74 (d, 4H, $J$ = 5.4 Hz, $bpy_{ex}$-6,6′), 8.32 (d, 4H, $J$ = 8.2 Hz, $bpy_{ex}$-3,3′), 8.20 (dd, 4H, $J$ = 8.2, 7.7 Hz, $bpy_{ex}$-4,4′), 8.04 (d, 2H, $J$ = 5.4 Hz, $bpy_{in}$-6,6′), 7.94 (d, 2H, $J$ = 8.2 Hz, $bpy_{in}$-3,3′), 7.88 (dd, 2H, $J$ = 8.2, 7.7 Hz, $bpy_{in}$-4,4′), 7.59 (dd, 4H, $J$ = 7.6, 5.6 Hz, $bpy_{ex}$-5,5′), 7.52 (m, 8H, Ph-*p*), 7.39 (m, 16H, Ph-*m*), 7.03 (dd, 2H, $J$ = 7.7, 5.4 Hz, $bpy_{in}$-5,5′), 6.95 (m, 16H, Ph-*o*), 5.91−5.72 (m, 4H, P—C*H*═C*H*—P) ppm. FT-IR ($CH_3CN$): $\nu$(CO) 2043, 1958, 1945 1926, 1874 cm$^{-1}$. ESI-MS ($CH_3CN$): $m/z$ 681 [M − $3PF_6$]$^{3+}$.

*[Re(bpy)(CO)$_3$\{($\eta^2$-vi)Re(bpy)(CO)$_2$\}$_2$($\eta^2$-vi)Re(bpy)(CO)$_3$](PF$_6$)$_4$* ***(L4vi)***. This complex was synthesized according to the same procedure as for **L4ph**. Starting from **L2vi** (200 mg, 0.13 mmol), and reacting with *trans*-bis(diphenylphosphino)ethylene (30 mg, 0.07 mmol) after the irradiation, the target **L4vi** was obtained as orange crystals (135 mg, 61%).

$^1$H NMR (400 MHz, $CD_3COCD_3$): $\delta$ 8.73 (d, 4H, $J$ = 5.4 Hz, $bpy_{ex}$-6,6′), 8.31 (d, 4H, $J$ = 8.2 Hz, $bpy_{ex}$-3,3′), 8.19 (dd, 4H, $J$ = 8.2, 7.7 Hz, $bpy_{ex}$-4,4′), 7.98 (d, 4H, $J$ = 5.4 Hz, $bpy_{in}$-6,6′), 7.93 (d, 4H, $J$ = 8.2 Hz, $bpy_{in}$-3,3′), 7.87 (dd, 4H, $J$ = 8.2, 7.7 Hz, $bpy_{in}$-4,4′), 7.57 (dd, 4H, $J$ = 7.7, 5.4 Hz, $bpy_{ex}$-5,5′), 7.55−7.27 (m, 36H, Ph-*p* + Ph-*m*), 7.01 (dd, 4H, $J$ = 7.7, 5.4 Hz, $bpy_{in}$-5,5′), 6.93 (m, 24H, Ph-*o*), 5.90−5.64 (m, 6H, P—C*H*═C*H*—P) ppm. FT-IR ($CH_3CN$): $\nu$(CO): 2043, 1957, 1943 1926, 1874 cm$^{-1}$. ESI-MS ($CH_3CN$) $m/z$ 710 [M − $4PF_6$]$^{4+}$.

**General Procedure for the Synthesis of R*nx*.** A degassed solution of the corresponding **L*nx*** (ca. 0.25 mM) in acetone−$H_2O$ mixture (7:1 v/v) was irradiated until the starting compound was consumed and both terminal CO ligands were substituted by solvent (2−8 h), as monitored by ESI-MS technique. The mixture was evaporated, and the residue was dissolved in $CH_3CN$ and evaporated to dryness (this procedure was repeated three times). The crude **L*nx*-($CH_3CN$)$_2$** was dissolved together with the corresponding phosphine ligand **P−P** (1.1 equiv) in acetone (ca. 3 mM) and refluxed under Ar in dim light for 24 h. Afterward, purification was carried out individually for each compound as described below.

*[{Re(bpy)(CO)$_2$($\eta^2$-ph)}$_3$](PF$_6$)$_3$* ***(R3ph)***. Starting from 140 mg of **L3ph** (0.05 mmol) and after following the general strategy, the reaction mixture was evaporated, and the crude material was purified by SEC. The fraction containing **R3ph** was collected, evaporated, and portioned between $CH_2Cl_2$ and a $NH_4PF_6$ aqueous solution. The organic layer was washed once more with an aqueous $NH_4PF_6$ solution, dried over $Na_2SO_4$, and evaporated. After short column chromatography ($SiO_2$, $CH_3CN$−$CH_2Cl_2$ 1:5), a final recrystallization from EtOH−$CH_2Cl_2$ yielded the desired compound as yellow crystals (76 mg, 47%).

$^1$H NMR (300 MHz, $CD_3CN$): $\delta$ 8.26 (br s, 12H, P−$C_6H_4$−P), 8.03 (d, 6H, $J$ = 8.4 Hz, bpy-3,3′), 7.95 (d, 6H, $J$ = 5.7 Hz, bpy-6,6′), 7.73 (dd, 6H, $J$ = 8.4, 7.8 Hz, bpy-4,4′), 7.19 (t, 12H, $J$ = 7.5 Hz, Ph-*p*), 7.10 (t, 24H, $J$ = 7.5 Hz, Ph-*m*), 6.96 (m, 24H, Ph-*o*), 6.75 (dd, 6H, $J$ = 7.8, 5.7 Hz, bpy-5,5′) ppm. $^{31}$P NMR (161 MHz): $\delta$ 22.5 (*P*−$C_6H_4$−*P*) ppm. FT-IR ($CH_3CN$): $\nu$(CO) 1938, 1880 cm$^{-1}$. ESI-MS ($CH_3CN$): $m/z$ 845 [M − $3PF_6$]$^{3+}$. Anal. Calcd (%) for $C_{126}H_{96}F_{18}N_6O_6P_9Re_3$: C, 50.96; H, 3.26; N, 2.83. Found: C, 50.71; H, 3.55; N, 2.76.

*[{Re(bpy)(CO)$_2$($\eta^2$-ph)}$_4$](PF$_6$)$_4$* ***(R4ph)***. Starting from 90 mg of **L4ph** (0.025 mmol) and after following the general strategy, the reaction mixture was cooled down, and the precipitate was filtered off. The solid was purified on short column chromatography ($SiO_2$, $CH_3CN$−$CH_2Cl_2$ 2:5), and a final recrystallization from $CH_3CN$−$H_2O$ afforded the desired compound as fine yellow crystals (7 mg, 7%).

$^1$H NMR (400 MHz, $CD_3CN$): $\delta$ 7.95 (d, 8H, $J$ = 8.0 Hz, bpy-3,3′), 7.89 (d, 8H, $J$ = 5.2 Hz, bpy-6,6′), 7.69 (dd, 8H, $J$ = 8.0, 7.6 Hz, bpy-4,4′), 7.39 (m, 16H, P−$C_6H_4$−P), 7.35 (t, 16H, $J$ = 7.6 Hz, Ph-*p*), 7.25 (t, 32H, $J$ = 7.6 Hz, Ph-*m*), 7.08 (m, 32H, Ph-*o*), 6.72 (dd, 8H, $J$ = 7.6, 5.4 Hz, bpy-5,5′) ppm. $^{31}$P NMR (161 MHz): $\delta$ 21.7 (*P*−$C_6H_4$−*P*) ppm. FT-IR ($CH_3CN$): $\nu$(CO) 1940, 1869 cm$^{-1}$. ESI-MS ($CH_3CN$): $m/z$ 845 [M − $4PF_6$]$^{4+}$. HRMS (ESI-TOFMS) ($CH_3CN$): $m/z$ [M − $4PF_6$]$^{4+}$ Calcd for $C_{168}H_{128}N_8O_8P_8Re_4$: 845.1497. Found: 845.1479.

*[{Re(bpy)(CO)$_2$($\eta^2$-vi)}$_3$](PF$_6$)$_3$* ***(R3vi)***. Starting from 150 mg of **L3vi** (0.06 mmol), following the general strategy and purification analogous to **R3ph**, the desired compound **R3vi** was obtained as fine yellow crystals (46 mg, 27%).

$^1$H NMR (400 MHz, $CD_3CN$): $\delta$ 8.55 (d, 6H, $J$ = 5.2 Hz, bpy-6,6′), 7.73 (dd, 6H, $J$ = 8.0, 7.6 Hz, bpy-4,4′), 7.60 (d, 6H, $J$ = 8.0 Hz, bpy-3,3′), 7.32 (t, 12H, $J$ = 7.6 Hz, Ph-*p*), 7.24 (dd, 6H, $J$ = 7.6, 5.6 Hz, bpy-5,5′), 7.18 (t, 24H, $J$ = 7.6 Hz, Ph-*m*), 6.80 (br, 24H, Ph-*o*), 6.01 (m, 6H, P—C*H*═C*H*—P) ppm. $^{31}$P NMR (161 MHz): $\delta$ 16.2 (*P*—$C_2H_2$—*P*) ppm. FT-IR ($CH_3CN$): $\nu$(CO) 1943, 1889 (sh), 1870 (sh), 1860 cm$^{-1}$. ESI-MS ($CH_3CN$): $m/z$ 795 [M − $3PF_6$]$^{3+}$. Anal. Calcd (%) for $C_{114}H_{90}F_{18}N_6O_6P_9Re_3$: C, 48.57; H, 3.22; N, 2.98. Found: C, 48.78; H, 3.44; N, 3.05.

*[{Re(bpy)(CO)$_2$($\eta^2$-vi)}$_4$](PF$_6$)$_4$* ***(R4vi)***. Starting from 100 mg of **L4vi** (0.03 mmol), following the general strategy and purification analogous to **R4ph**, the desired compound was obtained as fine yellow crystals (35 mg, 32%).

$^1$H NMR (400 MHz, $CD_3CN$): $\delta$ 7.86 (d, 8H, $J$ = 5.6 Hz, bpy-6,6′), 7.65−7.58 (m, 16H, bpy-4,4′ + bpy-3,3′), 7.40 (t, 16H, $J$ = 7.6 Hz, Ph-*p*), 7.27 (t, 32H, $J$ = 7.6 Hz, Ph-*m*), 6.85−6.78 (br, 40H, Ph-*o* + bpy-5,5′), 5.36 (m, 8H, P—C*H*═C*H*—P) ppm. $^{31}$P NMR (161 MHz): $\delta$ 16.8 (*P*—C*H*═C*H*—*P*) ppm. FT-IR ($CH_3CN$): $\nu$(CO) 1943, 1867 cm$^{-1}$. ESI-MS ($CH_3CN$): $m/z$ 795 [M − $4PF_6$]$^{4+}$. Anal. Calcd (%) for $C_{152}H_{120}F_{24}N_8O_8P_{12}Re_4$: C, 48.57; H, 3.22; N, 2.98. Found: C, 48.52; H, 3.01; N, 2.75.

*[{Re(bpy)(CO)$_2$($\eta^2$-ac)}$_3$](PF$_6$)$_3$* ***(R3ac)***. Starting from 220 mg of **L3ac** (0.089 mmol), following the general strategy and purification


DOI: 10.1021/acs.inorgchem.5b01397
*Inorg. Chem.* 2015, 54, 8769−8777

analogous to **R3ph**, the desired compound **R3ac** was obtained as fine yellow crystals (76 mg, 30%).

$^1$H NMR (400 MHz, $CD_3CN$): $\delta$ 8.83 (d, 6H, $J$ = 5.2 Hz, bpy-6,6′), 7.60 (t, 6H, $J$ = 8.0 Hz, bpy-4,4′), 7.47 (d, 6H, $J$ = 8.0 Hz, bpy-3,3′), 7.38 (t, 12H, $J$ = 7.6 Hz, Ph-*p*), 7.19 (m, 30H, bpy-5,5′ + Ph-*m*), 6.98 (dd, 24H, $J$ = 13.2 $\{^3J_{HP}\}$, 7.2 Hz, Ph-*o*) ppm. $^{13}$C NMR (100 MHz, $CD_3CN$): $\delta$ 201.0 (t, $^2J_{CP}$ = 8.0 Hz, *C*O), 155.2 (s, bpy-*C2,C2*′), 153.9 (s, bpy-*C6,C6*′), 139.8 (s, bpy-*C4,C4*′), 132.5 (s, Ph-$C_p$), 132.2 (t, $^3J_{CP}$ = 6.5 Hz, Ph-$C_m$), 130.2 (t, $^2J_{CP}$ = 5.3 Hz, Ph-$C_o$), 128.8 (s, bpy-*C3,C3*′), 128.4 (t, $^1J_{CP}$ = 26.1 Hz, Ph-$C_{ipso}$), 124.6 (s, bpy-*C5,C5*′), 103.4 (dd, $^1J_{CP}$ = 35.1, 32.8 Hz, P−C≡*C*−P) ppm. $^{31}$P NMR (161 MHz): $\delta$ 3.9 (*P*−C≡C−*P*) ppm. FT-IR ($CH_3CN$): $\nu$(CO) 1954, 1900 (sh), 1882, 1874 cm$^{-1}$. ESI-MS ($CH_3CN$): $m/z$ 793 $[M - 3PF_6]^{3+}$. Anal. Calcd (%) for $C_{114}H_{84}F_{18}N_6O_6P_9Re_3$: C, 48.67; H, 3.01; N, 2.99. Found: C, 48.89; H, 3.22; N, 3.15.

*[{Re(bpy)(CO)$_2$($\eta^2$-ac)}$_4$](PF$_6$)$_4$* (***R4ac***). Starting from 115 mg of **L4ac** (0.034 mmol), following the general strategy and purification analogous to **R4ph**, the desired compound **R4ac** was obtained as fine yellow crystals (55 mg, 44%).

$^1$H NMR (400 MHz, $CD_3CN$): $\delta$ 7.99 (d, 8H, $J$ = 5.4 Hz, bpy-6,6′), 7.43 (t, 16H, $J$ = 7.6 Hz, Ph-*p*), 7.37−7.24 (m, 40H, Ph-*m* + bpy-3,3′), 7.12 (dd, 8H, $J$ = 8.0, 7.6 Hz, bpy-4,4′), 7.01 (dd, 32H, $J$ = 13.2 $\{^3J_{HP}\}$, 7.2 Hz, Ph-*o*), 6.91 (dd, 8H, $J$ = 7.6, 5.6 Hz, bpy-5,5′) ppm. FT-IR ($CH_3CN$): $\nu$(CO) 1955, 1883 (sh), 1874 cm$^{-1}$. ESI-MS ($CH_3CN$): $m/z$ 793 $[M - 4PF_6]^{4+}$. Anal. Calcd (%) for $C_{152}H_{112}F_{24}N_8O_8P_{12}Re_4$: C, 48.67; H, 3.01; N, 2.99. Found: C, 48.46; H, 2.80; N, 2.97.

## ■ ASSOCIATED CONTENT

### Supporting Information

The Supporting Information is available free of charge on the ACS Publications website at DOI: 10.1021/acs.inorgchem.5b01397.

X-ray structures, crystallographic data and selected distances, bond lengths and angles, $^1$H NMR spectrum, cyclic and differential pulse voltammograms, and UV−vis absorption spectra (PDF)

X-ray crystallographic data of **R3ph**, **R3vi**, **R3ac**, and **R4ph** (CIF)

## ■ AUTHOR INFORMATION


### Corresponding Author

*E-mail: ishitani@chem.titech.ac.jp.


### Notes

The authors declare no competing financial interest.

## ■ ACKNOWLEDGMENTS

Financial support by Grant-in-Aid for Scientific Research on Innovative Areas “Artificial Photosynthesis (AnApple)” (Grant 24107005) of Japan Society for the Promotion of Science is gratefully acknowledged.

## ■ REFERENCES


(1) Vlček, A. *Coord. Chem. Rev.* **1998**, *177*, 219−256.

(2) *Photochemistry and Photophysics of Coordination Compounds I*; Balzani, V., Campagna, S., Eds.; Springer: Berlin, 2007; Vol. *280*.

(3) *Photochemistry and Photophysics of Coordination Compounds II*; Balzani, V., Campagna, S., Eds.; Springer: Berlin, 2007; Vol. *281*.

(4) *Photofunctional Transition Metal Complexes*; Yam, V. W. W., Ed.; Springer: Berlin, 2007; Vol. *123*.

(5) *Molecular Organometallic Materials for Optics*; Bozec, H., Guerchais, V., Eds.; Springer: Berlin, 2010; Vol. *28*.

(6) Wrighton, M.; Morse, D. L. *J. Am. Chem. Soc.* **1974**, *96*, 998−1003.

(7) Vogler, A.; Kunkely, H. *Coord. Chem. Rev.* **2000**, *200−202*, 991−1008.

(8) Vlček, A. In *Photophysics of Organometallics*; Lees, A. J., Ed.; Topics in Organometallic Chemistry; Springer: Berlin, 2009; Vol. *29*, pp 115−158.

(9) Sato, S.; Ishitani, O. *Coord. Chem. Rev.* **2015**, *282−283*, 50−59.

(10) Koike, K.; Tanabe, J.; Toyama, S.; Tsubaki, H.; Sakamoto, K.; Westwell, J. R.; Johnson, F. P. A.; Hori, H.; Saitoh, H.; Ishitani, O. *Inorg. Chem.* **2000**, *39*, 2777−2783.

(11) Tsubaki, H.; Sekine, A.; Ohashi, Y.; Koike, K.; Takeda, H.; Ishitani, O. *J. Am. Chem. Soc.* **2005**, *127*, 15544−15555.

(12) Morimoto, T.; Ito, M.; Koike, K.; Kojima, T.; Ozeki, T.; Ishitani, O. *Chem. - Eur. J.* **2012**, *18*, 3292−3304.

(13) Balzani, V.; Moggi, L.; Scandola, F. In *Supramolecular Photochemistry*; Springer: Dordrecht, The Netherlands, 1987; pp 1−28.

(14) Balzani, V.; Juris, A.; Venturi, M.; Campagna, S.; Serroni, S. *Chem. Rev.* **1996**, *96*, 759−833.

(15) Liu, Y.; Li, Y.; Schanze, K. S. *J. Photochem. Photobiol., C* **2002**, *3*, 1−23.

(16) Happ, B.; Winter, A.; Hager, M. D.; Schubert, U. S. *Chem. Soc. Rev.* **2012**, *41*, 2222−2255.

(17) Yamamoto, Y.; Sawa, S.; Funada, Y.; Morimoto, T.; Falkenström, M.; Miyasaka, H.; Shishido, S.; Ozeki, T.; Koike, K.; Ishitani, O. *J. Am. Chem. Soc.* **2008**, *130*, 14659−14674.

(18) Yamamoto, Y.; Tamaki, Y.; Yui, T.; Koike, K.; Ishitani, O. *J. Am. Chem. Soc.* **2010**, *132*, 11743−11752.

(19) Yamamoto, Y.; Takeda, H.; Yui, T.; Ueda, Y.; Koike, K.; Inagaki, S.; Ishitani, O. *Chem. Sci.* **2014**, *5*, 639−648.

(20) Morimoto, T.; Nishiura, C.; Tanaka, M.; Rohacova, J.; Nakagawa, Y.; Funada, Y.; Koike, K.; Yamamoto, Y.; Shishido, S.; Kojima, T.; Saeki, T.; Ozeki, T.; Ishitani, O. *J. Am. Chem. Soc.* **2013**, *135*, 13266−13269.

(21) Asatani, T.; Nakagawa, Y.; Funada, Y.; Sawa, S.; Takeda, H.; Morimoto, T.; Koike, K.; Ishitani, O. *Inorg. Chem.* **2014**, *53*, 7170−7180.

(22) Koike, K.; Okoshi, N.; Hori, H.; Takeuchi, K.; Ishitani, O.; Tsubaki, H.; Clark, I. P.; George, M. W.; Johnson, F. P. A.; Turner, J. J. *J. Am. Chem. Soc.* **2002**, *124*, 11448−11455.

(23) Takeda, H.; Yamamoto, Y.; Nishiura, C.; Ishitani, O. *Anal. Sci.* **2006**, *22*, 545−549.

(24) Caspar, J. V.; Sullivan, B. P.; Meyer, T. J. *Inorg. Chem.* **1984**, *23*, 2104−2109.

(25) We observed only broadening of the signals in the low-temperature $^1$H NMR spectra of **R3ac**, measured either in $CD_3CN$ up to −40 °C, or in acetone-$d_6$ up to −80 °C.

(26) Morrison, S. L.; Turner, J. J. *J. Mol. Struct.* **1994**, *317*, 39−47.

(27) Caspar, J. V.; Meyer, T. J. *J. Phys. Chem.* **1983**, *87*, 952−957.

(28) Van Calcar, P. M.; Olmstead, M. M.; Balch, A. L. *Inorg. Chim. Acta* **1998**, *270*, 28−33.

(29) Sheldrick, G. M. *Acta Crystallogr., Sect. A: Found. Crystallogr.* **2008**, *64*, 112−122.

(30) Sheldrick, G. M. *Acta Crystallogr., Sect. A: Found. Adv.* **2015**, *71*, 3−8.

(31) Suzuki, K.; Kobayashi, A.; Kaneko, S.; Takehira, K.; Yoshihara, T.; Ishida, H.; Shiina, Y.; Oishi, S.; Tobita, S. *Phys. Chem. Chem. Phys.* **2009**, *11*, 9850−9860.




DOI: 10.1021/acs.inorgchem.5b01397
*Inorg. Chem.* 2015, 54, 8769−8777